

# The Structure and Interactions of the Proline-rich Domain of ASPP2<sup>\*[S]</sup>

Received for publication, October 22, 2007, and in revised form, April 30, 2008. Published, JBC Papers in Press, April 30, 2008, DOI 10.1074/jbc.M708717200

Shahar Rotem<sup>‡</sup>, Chen Katz<sup>‡</sup>, Hadar Benyamini<sup>‡</sup>, Mario Lebendiker<sup>§</sup>, Dmitry Veprintsev<sup>¶</sup>, Stefan Rüdiger<sup>||</sup>, Tsafi Danieli<sup>§</sup>, and Assaf Friedler<sup>‡2</sup>

From the <sup>‡</sup>Institute of Chemistry, <sup>§</sup>Protein Expression and Purification Facilities, The Wolfson Centre for Applied Structural Biology, The Hebrew University of Jerusalem, Safra Campus, Givat Ram, Jerusalem 91904, Israel, the <sup>¶</sup>MRC Laboratory of Molecular Biology, Hills Road, Cambridge CB2 0QH, United Kingdom, and <sup>||</sup>Cellular Protein Chemistry, Bijvoet Center for Biomolecular Research, Utrecht University, Padualaan 8, 3584 CH Utrecht, The Netherlands

ASPP2 is a pro-apoptotic protein that stimulates the p53-mediated apoptotic response. The C terminus of ASPP2 contains ankyrin (Ank) repeats and a SH3 domain, which mediate its interactions with numerous partner proteins such as p53, NFκB, and Bcl-2. It also contains a proline-rich domain (ASPP2 Pro), whose structure and function are unclear. Here we used biophysical and biochemical methods to study the structure and the interactions of ASPP2 Pro, to gain insight into its biological role. We show, using biophysical and computational methods, that the ASPP2 Pro domain is natively unfolded. We found that the ASPP2 Pro domain interacts with the ASPP2 Ank-SH3 domains, and mapped the interaction sites in both domains. Using a combination of peptide array screening, biophysical and biochemical techniques, we found that ASPP2 Ank-SH3, but not ASPP2 Pro, mediates interactions of ASPP2 with peptides derived from its partner proteins. ASPP2 Pro-Ank-SH3 bound a peptide derived from its partner protein NFκB weaker than ASPP2 Ank-SH3 bound this peptide. This suggested that the presence of the proline-rich domain inhibited the interactions mediated by the Ank-SH3 domains. Furthermore, a peptide from ASPP2 Pro competed with a peptide derived from NFκB on binding to ASPP2 Ank-SH3. Based on our results, we propose a model in which the interaction between the ASPP2 domains regulates the intermolecular interactions of ASPP2 with its partner proteins.

ASPP2 (see Fig. 1A) is one of three members of the ASPP (apoptosis-stimulating proteins of p53)<sup>3</sup> family, which specifically stimulates the apoptotic response mediated by the tumor

suppressor protein p53 (1). Human ASPP2 is a 1128-amino acid protein, whose C-terminal part (amino acids (aa) 600–1128) was originally identified as a protein that binds the p53 core domain and was named p53-binding protein 2 (53BP2) (2). Another truncated form of ASPP2 (aa 123–1128) was discovered as Bbp (Bcl-2-binding protein) (3) (Fig. 1A). Full-length ASPP2 was found to specifically stimulate the apoptotic function of p53 by enhancing the transactivation function of p53 on the promoters of pro-apoptotic genes, but it has no effect on genes involved in cell cycle arrest (1). ASPP2 contains several structural and functional domains (Fig. 1A): Its N terminus (residues 1–83) has the structure of a β-Grasp ubiquitin-like fold (4). It is followed by a predicted α-helical domain located between aa 123 and 323 (3), and a proline-rich (ASPP2 Pro) domain between aa 674 and 902 (3). The C-terminal part of ASPP2 contains four ankyrin repeats and an SH3 domain (ASPP2 Ank-SH3), as seen from its crystal structure in complex with p53 core domain (5). The crystal structure of the C-terminal domain of the homologous ASPP family member iASPP was solved recently, showing a similar structure of four ankyrin repeats and an SH3 domain. The C-terminal domain of iASPP formed a homodimer mediated by contacts between the N-terminal part of one molecule and the SH3 domain and the third ankyrin repeat of a second molecule (6). The ASPP2 Ank-SH3 domains mediate the interactions of ASPP2 with numerous partner proteins, most of which are involved in apoptosis or its regulation. Among these partner proteins are p53 (2), the anti-apoptotic protein Bcl-2 (3), the p65 subunit of the transcription factor NFκB (7), protein phosphatase 1 (8), the pro-apoptotic Yes-associated protein 1 (YAP1) (9), the N-terminal 46 residues of the hepatitis C virus (HCV) core protein (10), and the p53 tumor suppressor family members p63 and p73 (11). The role of the ASPP2 Pro domain is unclear. This domain was not shown to bind other proteins, with the only exception being the interaction with YAP1. This interaction is mediated predominantly via the ASPP2 SH3 domain, but there is an additional binding site in the C terminus of the ASPP2 Pro domain, which is adjacent to the ASPP2 Ank-SH3 domains (9).

Peptides are valuable experimental tools to study proteins in many cases. This is particularly useful in the case of natively unfolded protein domains: Peptides, which are in most cases also unstructured, are excellent tools to study such domains. Peptides are also good models for binding studies, because they may gain their native structure upon ligand binding. This was

\* This work was supported in part by a career development award from the Human Frontier Science Program Organization, by an Excellence Grant from the Israel Cancer Association (to A. F.), and by a Lady Davis fellowship (to H. B.). The costs of publication of this article were defrayed in part by the payment of page charges. This article must therefore be hereby marked "advertisement" in accordance with 18 U.S.C. Section 1734 solely to indicate this fact.

[S] The on-line version of this article (available at <http://www.jbc.org>) contains supplemental Tables S1–S3.

<sup>1</sup> Supported by a Marie Curie Excellence Grant of the European Union, a VIDI grant of the Netherlands Science Organization and the High Potential program of Utrecht University.

<sup>2</sup> To whom correspondence should be addressed: Tel.: 972-2-658-5746; Fax: 972-2-658-5345; E-mail: [assaf@chem.ch.huji.ac.il](mailto:assaf@chem.ch.huji.ac.il).

<sup>3</sup> The abbreviations used are: ASPP, apoptosis-stimulating proteins of p53; aa, amino acid(s); YAP1, Yes-associated protein 1; HCV, hepatitis C virus; NTA, nitrilotriacetic acid; HLT, HislipoteV; IS, ionic strength; AUC, analytical ultracentrifugation; Ank, ankyrin; TEV, tobacco etch virus.

shown for example for peptides derived from the BH4 domain of Bcl-2 (12) and from the pro-apoptotic Bak (13). Peptides are also useful to map interaction sites between proteins: Peptide arrays provide a highly efficient way for identifying the location of the binding sites in both interaction partners (14). There have been numerous applications of peptide arrays for the study of epitope mapping, enzyme binding, and protein-protein interactions (15–19). Here we used peptides to gain information about the structure and interactions of ASPP2 domains using both methodologies: peptides as models for the ASPP2 Pro domain, which we found to be natively unfolded (see below), and peptide arrays to identify the precise binding sites involved in intramolecular and intermolecular interactions of ASPP2.

Our aim in the current study was to elucidate the structure and the interactions of the ASPP2 Pro domain to gain insight into its function. Our results show that the ASPP2 Pro domain is natively unfolded. We found that ASPP2 Pro makes an interaction with the ASPP2 Ank-SH3 domains and mapped the interaction sites in both domains. However, according to our results ASPP2 Pro does not mediate the interactions of ASPP2 with peptides derived from its partner proteins. ASPP2 Pro-Ank-SH3 bound a peptide derived from its partner protein NF $\kappa$ B weaker than ASPP2 Ank-SH3 bound this peptide. This suggested that the presence of the proline-rich domain inhibited the interactions mediated by the Ank-SH3 domains. This was confirmed by our observation that a peptide from ASPP2 Pro competed with a peptide derived from NF $\kappa$ B on binding to ASPP2 Ank-SH3. Based on our results, we propose a model in which the interaction between the ASPP2 domains regulates the intermolecular interactions of ASPP2 with its partner proteins.

## EXPERIMENTAL PROCEDURES

**Expression Plasmids**—The constructs pRHisLipoTEV (pHLT) ASPP2 Ank-SH3, containing ASPP2 893–1128 was a kind gift of Dr. Mark Allen, Cambridge, UK. The construct pGEX2TK ASPP2 Pro-Ank-SH3, containing ASPP2 693–1128 amino acids was a kind gift from Prof. Xin Lu, Ludwig Institute for Cancer Research, London, UK. Point mutations were introduced into the gene encoding ASPP2 using the Site-Direct Mutagenesis kit (iNtRON). The construct pHLT ASPP2 Pro-Ank-SH3 was obtained by cloning of the ASPP2 693–1128 fragment from pGEX2TK ASPP2 Pro-Ank-SH3 into the pHLT ASPP2 Ank-SH3 construct. This was done in the following manner: pGEX2TK ASPP2 Pro-Ank-SH3 vector was restricted with BamHI and PstI enzymes. The fragment from this reaction was then used to replace the original BamHI-PstI fragment in the pHLT ASPP2 Ank-SH3, creating pHLT ASPP2 Pro-Ank-SH3. The truncated form pHLT ASPP2 Pro containing ASPP2 amino acids 693–918 was obtained by introducing two stop codons in positions 919 and 920 on the pHLT ASPP2 Pro-Ank-SH3 template, using site-directed mutagenesis with the following oligonucleotides: (i) 5'-GGCTCAGAGCGTATCGCTCATTAATAGAGGGTGAAT-TCAACCCC-3'; (ii) 5'-GGGGTTGAATTCACCCTCTA-TTAATGAGCGATACGCTCTGAGCC-3'. All constructs were

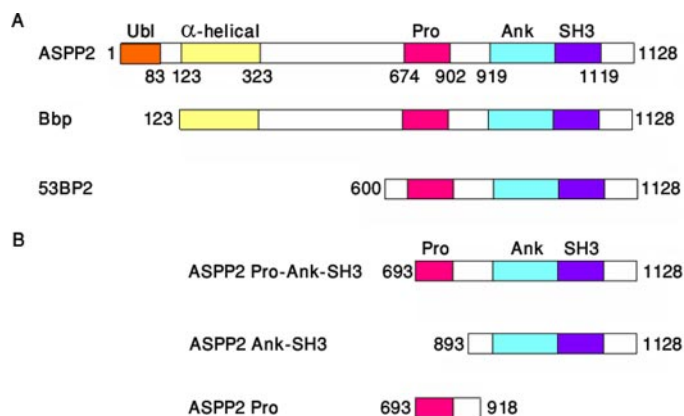


FIGURE 1. **ASPP2 and its truncated forms.** A, ASPP2 and its truncated forms Bbp and p53-binding protein 2 (53BP2) all contain a proline-rich domain (Pro), four ankyrin repeats (Ank), and an SH3 domain. ASPP2 and Bbp also contain a putative  $\alpha$ -helical domain at their N terminus (1, 3, 5). The N-terminal part of ASPP2 has the structure of a  $\beta$ -Grasp ubiquitin-like fold (Ubl) (4). B, the different recombinant truncated ASPP2 constructs that were used in the current study.

verified by DNA sequence analysis (Center for Genomic Technologies, the Hebrew University).

**Protein Expression and Purification**—We expressed and purified three truncated ASPP2 variants with and without the HLT tag containing His tag, Lipo domain, and TEV protease cleavage site (20) (Fig. 1B). All pHLT constructs were expressed in *Escherichia coli* BL21 pLysS cells (Novagen). Cells were grown in 2 $\times$  YT media containing 1% glucose. Induction was done at  $A_{600\text{ nm}} = 0.6$  with 0.1 mM isopropyl  $\beta$ -D-thiogalactopyranoside for the pHLT ASPP2 Pro and for pHLT ASPP2 Pro-Ank-SH3, and with 1 mM isopropyl  $\beta$ -D-thiogalactopyranoside for pHLT ASPP2 Ank-SH3. All cells were harvested after 14-h incubation at 22  $^{\circ}$ C for constructs ASPP2 Ank-SH3 and ASPP2 Pro and 16  $^{\circ}$ C for construct ASPP2 Pro-Ank-SH3.

**Purification of ASPP2 Pro-Ank-SH3**—Cells were lysed by French Pressure cell press (SIM-AMINCO) and purified on a nickel-Sepharose HP column (Amersham Biosciences) using an ÄKTA explorer system (Amersham Biosciences). The protein was eluted using imidazole. The eluted protein was digested overnight at 24  $^{\circ}$ C with His-tagged TEV protease (21) and further purified on a Superdex 200 column (Amersham Biosciences). Eluted protein was further purified on nickel-NTA beads (Qiagen) to trap the His-tagged TEV protease and residual uncleaved protein.

**Purification of ASPP2 Pro**—Cells were lysed by French Pressure cell press and purified on a nickel-Sepharose HP column using an ÄKTA explorer system. The protein was eluted using imidazole. The protein was further purified on Superose 12 (Amersham Biosciences). Part of the protein was aliquoted and stored at  $-80^{\circ}$  C; the rest of the sample was digested overnight at 24  $^{\circ}$ C with His-tagged TEV protease (21) and further purified on a 10-ml nickel-NTA column (Qiagen) to trap the His-tagged TEV protease, the HLT tag, and residual uncleaved protein.

**Purification of ASPP2 Ank-SH3**—Cells were lysed by microfluidizer processor M-110EHI and purified a nickel-Sepharose HP column using an ÄKTA explorer system. The protein was eluted using imidazole. The protein was further purified on Resource Q30 column (Amersham Biosciences)

## Domain-Domain Interaction in ASPP2

and eluted by NaCl gradient. The eluted protein was digested overnight at 30 °C with His-TEV protease (21) and subsequently reapplied onto the nickel-NTA column (Qiagen) to separate the His-tagged TEV protease and residual uncleaved protein. The unbound fraction was further purified on a Sephacryl S-100 column (Amersham Biosciences).

**Analytical Size Exclusion Chromatography**—HisipoTEV (HLT) 350  $\mu$ l of ASPP2 Pro at 4.1  $\mu$ M was injected to an analytical gel filtration Superose 12 (300  $\times$  10 mm) column, on an ÄKTA design Explorer instrument equipped with a Monitor UV-900 detector and the Unicorn software package. The running buffer was 20 mM phosphate buffer, pH 7.0, 150 mM NaCl, 10% glycerol at 4 °C. 150  $\mu$ l of 86  $\mu$ M ASPP2 Ank-SH3 was separated in 1-ml fractions from an analytical Superose 12 (300  $\times$  10 mm) column equilibrated with 25 mM phosphate buffer with 150 mM NaCl, at 4 °C. Molecular mass standards were run under the same conditions, and their elution volumes were used to create a calibration curve. The markers were: thyroglobin (669 kDa), ferritin (440 kDa), catalase (232 kDa),  $\beta$ -amylase (200 kDa), aldolase (163 kDa), bovine serum albumin (67 kDa), ovalbumin (44 kDa), and RNase A (13.7 kDa).

**Peptide Array Screening**—The peptide arrays were synthesized by Jerini Bio Tools GmbH (Berlin). The peptides were acetylated at their N terminus and attached to cellulose via their C terminus by an amide bond. Binding of the human ASPP2 893–1128 (ASPP2 Ank-SH3) to the cellulose-bound peptides was screened as described previously (17) with the following modifications: The peptide array was prewashed in binding buffer (30 mM Tris-HCl, pH 7.6, 0.075 M NaCl, 5 mM MgCl<sub>2</sub>, 5% sucrose, 0.05% Tween 20). ASPP2 Ank-SH3 in a final concentration of 6.8  $\mu$ M or ASPP2 Pro (final concentration, 1.4  $\mu$ M) was incubated with the array in binding buffer overnight at 4 °C with gentle shaking. The electrotransfer was performed in four steps: 10-min transfer followed by replacement of the polyvinylidene difluoride membrane and continuation of the transfer for additional 30 min; afterward all the “sandwiched” (blotting paper and polyvinylidene difluoride membrane) was replaced, and the transfer was continued for two more 30-min intervals. Transferred ASPP2 was detected using enhanced chemifluorescence with ASPP2-specific polyclonal rabbit antisera for ASPP2 Ank-SH3 and a different polyclonal rabbit antisera (a kind gift from Prof. Xin Lu) for ASPP2 Pro. Alternatively, a chemiluminescence blotting substrate Super Signal reagent (Pierce) was used according to the manufacturer’s instructions for detection using ECL.

**Nickel-affinity Pulldown Assay**—59  $\mu$ l of 45  $\mu$ M ASPP2 Ank-SH3 was incubated for 1 h with gentle agitation at 4 °C with 500  $\mu$ l of 5.3  $\mu$ M HLT ASPP2 Pro in 25 mM NaH<sub>2</sub>PO<sub>4</sub>, 150 mM NaCl, 10% glycerol, and with 500- $\mu$ l wash buffer (20 mM Tris-HCl, pH 7.0, with 150 mM NaCl, 10% glycerol, and 10 mM imidazole) alone. 20  $\mu$ l of nickel-NTA beads (Qiagen) equilibrated with wash buffer was added, and the incubation continued for another 1 h. The samples were centrifuged for 4 min at 3500 rpm at 4 °C, and the suspension was collected and defined as unbound. Samples were centrifuged, unbound material was collected, and beads were washed five times with buffer before elution with buffer containing 250 mM imidazole. Finally, samples were analyzed on a 12% SDS-PAGE gel.

**CD**—CD spectra were recorded using a J-810 spectropolarimeter (Jasco) in 5 mM phosphate buffer, pH 7.5, 30 mM NaCl, and 2% glycerol in a 0.1-cm quartz cuvette for far-UV CD spectroscopy. Far-UV CD spectra were collected in a spectral range of 185 to 250 nm. The changes in CD spectra with temperature were measured in a temperature range of 20–90 °C in 10 °C steps. Prior to each experiment ASPP2 Pro was centrifuged in 13,200 rpm for 10 min at 4 °C, and the UV spectrum between 200 and 400 nm was measured. The amount of secondary structure was analyzed using DichroWeb (22) with K2D software.

**Peptide Synthesis and Purification**—Peptides were synthesized on Applied Biosystems (ABI) 433A peptide synthesizer using standard *N*-(9-fluorenyl)methoxycarbonyl chemistry as described before (23).

**Fluorescein Labeling**—The peptides were labeled using 5' (and 6')-carboxyfluorescein succinimidyl ester (Molecular Probes) at the N terminus as described before (23).

**Fluorescence Anisotropy**—Measurements were performed at 10 °C by using a PerkinElmer Life Sciences LS-50b spectrofluorometer equipped with a Hamilton microlab M dispenser (24, 25). Titration of ASPP2 Ank-SH3 into the fluorescein-labeled peptides was performed in 20 mM Hepes at pH 7.3 with ionic strength (IS) of 50 mM, 100 mM, and 150 mM. Titration of ASPP2 Ank-SH3 and of ASPP2 Pro-Ank-SH3 into the fluorescein-labeled NF $\kappa$ B 303–332 was performed in 20 mM NaH<sub>2</sub>PO<sub>4</sub> at pH 7.0 with an IS of 50 mM. Fluorescence was measured with excitation at 480 nm and emission at 530 nm. The bandwidths were changed depending on the amount of the labeled molecule used. The labeled peptide was placed in the cuvette in a volume of 1 ml, at a concentration of 100 nM, and 150–200  $\mu$ l of ASPP2 Ank-SH3 was placed in the dispenser. Additions of 5  $\mu$ l were titrated at 90-s intervals, the solution was stirred for 10 s, and the fluorescence and anisotropy were measured. Dissociation constants ( $K_d$ ) were calculated by fitting the anisotropy titration curves (corrected for the dilution effect) by using Kaleidagraph (Synergy Software, Reading, PA). The following equation was used for the single-site model,

$$r = r_0 + \frac{r_a[\text{ASPP2 Ank-SH3}]}{K_d + [\text{ASPP2 Ank-SH3}]} \quad (\text{Eq. 1})$$

Where,  $r_0$  is the initial anisotropy,  $r_a$  is the difference in anisotropy between unbound and bound anisotropy,  $K_d$  is the dissociation constant, [ASPP2 Ank-SH3] is the molar concentration of ASPP2 Ank-SH3. Each experiment was performed at least three times, and  $K_d$  values were always reproducible. The experimental errors for  $K_d$  values are the result of the data fitting.

In the different competition binding assays, the conditions were as following: 150  $\mu$ l of 750  $\mu$ M ASPP2 723–737 was added to a 1150- $\mu$ l mixture of 87 nM fluorescein-labeled NF $\kappa$ B 303–332 and 2  $\mu$ M ASPP2 Ank-SH3 at 50 mM IS; 150  $\mu$ l of 195  $\mu$ M NF $\kappa$ B 303–332 was added to a 1150- $\mu$ l mixture of 87 nM fluorescein-labeled ASPP2 723–737 and 10.5  $\mu$ M ASPP2 Ank-SH3 at 50 mM IS; 100  $\mu$ l of 1500  $\mu$ M ASPP2 723–737 was added to a 1200- $\mu$ l mixture of 83 nM fluorescein-labeled ASPP2 723–737 and 26.5  $\mu$ M ASPP2 Ank-SH3 at 150 mM IS.

**Disorder Predictions**—We have used the following servers for disorder prediction for ASPP2: NORS (26), Disopred (27), PONDR (28), GlobPlot (29), RONN (30), PreLink (31), IUPred (32), SEG (33), DisPro (34), Disprot (35), and FoldIndex (36). In all cases, the whole sequence of ASPP2 (SP: ASPP2\_HUMAN) was subjected to disorder prediction using default server parameters.

**Cross-linking**—ASPP2 Pro-Ank-SH3 and ASPP2 Ank-SH3 (3.75  $\mu\text{M}$  final concentration) were incubated at 37 °C for 30 min in a pH 7.0 buffer containing 20 mM  $\text{NaH}_2\text{PO}_4$ , 110 mM NaCl, 5 mM  $\beta$ -mercaptoethanol, and 10% glycerol. The reaction mixtures were treated with the cross-linking agent BS3 (25, 50, or 100 eq, Pierce) for 30 min at 37 °C. The reaction mixtures were denatured and analyzed by 10% SDS-PAGE (37, 38).

**Analytical Ultracentrifugation**—AUC experiments were performed at 10 °C using a Beckman Optima XLI analytical ultracentrifuge with an An60Ti rotor. A 2.9  $\mu\text{M}$  sample of ASPP2 Pro-Ank-SH3 (693–1128) was subject to sedimentation equilibrium experiments. The buffer was 25 mM  $\text{NaH}_2\text{PO}_4$ , pH 7.0, 150 mM NaCl, 10% glycerol, 0.02%  $\text{NaN}_3$ , and 10 mM  $\beta$ -mercaptoethanol. Samples were loaded in triplicate into 6-sector 12-mm path length cells. Data were analyzed using the UltraSpin software. Data were fit to a single exponential model indicating equilibrium of single species of unspecified mass.

## RESULTS

**ASPP2 Pro Domain Is Natively Unfolded**—We used analytical size-exclusion chromatography to study the oligomerization state and compactness of the ASPP2 variants. ASPP2 Pro (aa 693–918) and ASPP2 Ank-SH3 (aa 893–1128) both eluted from the gel-filtration column as single peaks, indicating the existence of a single oligomeric form in both cases. The ASPP2 Pro domain eluted earlier than predicted from its molecular mass, and its apparent molecular mass estimated from the calibration curve was  $\sim 130,000$  Da (Fig. 2A), a value five times higher than the theoretical value of 24,500 Da. This early elution in the gel filtration may be attributed to an extended or unfolded native structure of the protein (39) or to putative oligomerization. The structured ASPP2 Ank-SH3 eluted as expected from its molecular weight. For this protein, the calculated and the estimated molecular mass were the same, with a value of 26,600 Da (Fig. 2B).

To determine the basis for the early elution of ASPP2 Pro in the gel filtration experiments, we analyzed its secondary structure using CD spectroscopy. The far-UV CD spectrum of the recombinant purified protein exhibited a minimum at only  $\sim 200$  nm (Fig. 3A), suggesting a highly unstructured conformation. To further test this, we monitored changes in the far-UV CD signal as a function of temperature (Fig. 3B). No change in the signal was observed, indicating no structural transition upon temperature increase. This is typical for unstructured proteins (40). Taken together, the CD spectra indicate a high content of unstructured regions in ASPP2 Pro domain.

We used computational methods to verify whether ASPP2 Pro is unstructured. We have submitted the sequence of ASPP2 to twelve publicly available servers that implement algorithms for protein disorder prediction (26–36, 41). These algorithms are based on different criteria to predict disordered conforma-

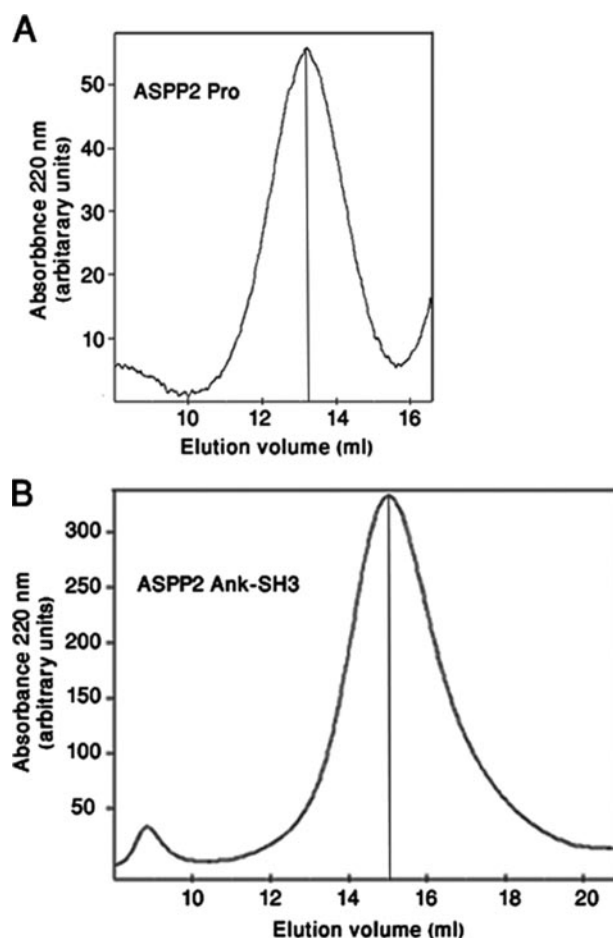


**FIGURE 2. Determination of the quaternary structure of ASPP2 Pro.** Analytical gel filtration studies of ASPP2 Pro compared with ASPP2 Ank-SH3 domains supports its lack of structure: *A*, ASPP2 Pro: The calculated molecular mass of ASPP2 Pro is 24,500 Da, but the experimental molecular mass estimated from the calibration curve corresponds to  $\sim 130,000$  Da. *B*, ASPP2 Ank-SH3: ASPP2 Ank-SH3 eluted after 15 ml, as expected from its calculated molecular mass of around 27,000 Da.

tion from sequence, as reviewed in Ferron *et al.* (41). In all cases we submitted the full-length ASPP2 sequence (1128 aa) and used the default parameters. The C-terminal part of ASPP2 (926–1128) is known to be structured (5) and thus served as a positive control for the disorder prediction. The results show that the sequence of the ASPP2 Pro domain is predicted to be disordered, whereas the sequence of residues 918–1128, which contains the Ank-SH3 domains, is predicted to be folded, as expected, by the different prediction methods (Fig. 3C). 57% of the amino acids in ASPP2 693–918 (ASPP2 Pro) are typical for disordered regions (Glu, Lys, Arg, Gly, Gln, Ser, and Pro) (42–44) (Fig. 3D), compared with only 34% in the ASPP2 Ank-SH3 domains. On the other hand, the amino acids Ile, Leu, Val, Trp, Phe, Tyr, Cys, and Asn, which are not favored in disordered regions, make only up to 27% of the ASPP2 Pro domain sequence. Together, our results imply that the ASPP2 Pro domain is highly unstructured with an extended conformation.

**Domain-Domain Interaction between ASPP2 Pro and ASPP2 Ank-SH3**—Proline-rich domains are known to serve as binding regions for SH3 domains (45, 46). This raised the possibility of a putative domain-domain interaction between the proline-rich and Ank-SH3 domains of ASPP2. We performed a nickel-affin-

## Domain-Domain Interaction in ASPP2

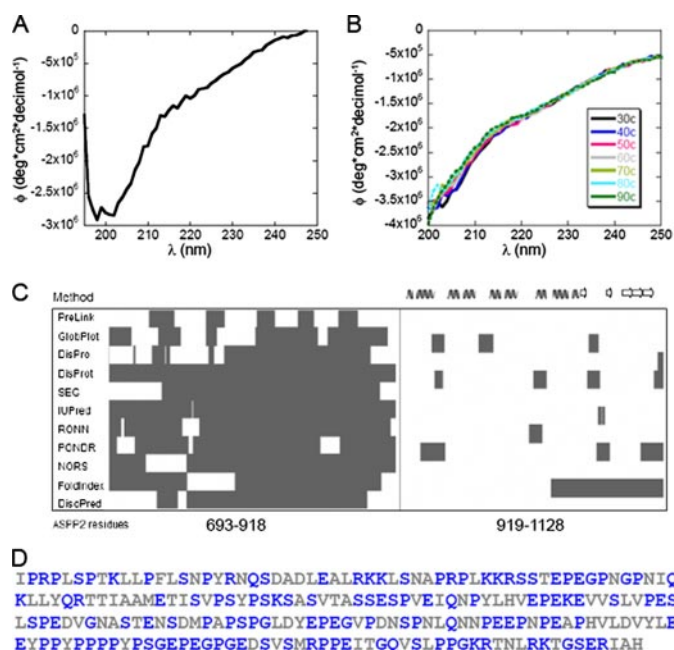


**FIGURE 3. Analysis of the structure of ASPP2 Pro by CD spectroscopy and computational predictions.** *A*, far-UV CD spectra of ASPP2 Pro. The spectrum almost lacks the typical signatures of secondary structure and exhibits a minimum around 200 nm, indicating an unfolded conformation. Analysis of the CD spectrum using the DichroWeb server (22) showed that ~40% of the protein corresponds to a random coil. *B*, temperature dependence of the CD spectrum of ASPP2 Pro. Spectra were measured at the range of 30–90 °C at 10 °C intervals. The lack of significant changes in the spectrum indicates the lack of a structural transition upon increase of the temperature, pointing again at an unstructured conformation. *C*, disorder predictions for residues 693–1128 of ASPP2. Each line represents the disorder prediction for the ASPP2 sequence by different methods (see “Experimental Procedures” for details). Segments that are predicted to be disordered are gray. The secondary structure for residues 919–1128, containing the ankyrin repeats and SH3 domains, is depicted in helices and arrows for  $\alpha$ -helices and  $\beta$ -strands, respectively. The different methods predict an unstructured conformation for the proline-rich region and a folded conformation for the ASPP2 Ank-SH3 region. *D*, the ASPP2 Pro sequence. 57% of the amino acids in ASPP2 Pro are typical for disordered regions (Glu, Lys, Arg, Gly, Gln, Ser, and Pro (colored blue) (42–44).

ity pull-down experiment to test whether the two domains interact with each other. ASPP2 Ank-SH3 was retrieved by nickel beads following its incubation with His-tagged ASPP2 Pro but not when incubated with the nickel beads alone (Fig. 4A). To confirm this observation, we performed cross-linking experiments. Incubation of ASPP2 Pro-Ank-SH3 with different concentrations of the cross-linker BS3 resulted in a protein that is mostly monomeric, but also in the formation of a small amount of dimers (Fig. 4B) and higher order oligomers (not shown). The formation of the higher order oligomers was dependent on the cross-linker BS3 concentration. We assume that most protein remained monomeric following the cross-linking due to a possible intramolecular cross-linking between the domains within each monomer. A different cross-linking experiment between ASPP2 Pro-Ank-SH3 and ASPP2 Ank-SH3 resulted in a similar pattern: most proteins remained monomeric, but the formation of two types of dimers was observed (Fig. 4C), attributed to cross-linked ASPP2 Pro-Ank-SH3–ASPP2 Pro-Ank-SH3 and ASPP2 Pro-Ank-SH3–ASPP2 Ank-SH3. Cross-linking experiments with ASPP2 Pro failed because the protein is very unstable and aggregated at the conditions required for the

experiment. Taken together, our data suggest that the proline-rich domain of ASPP2 is necessary for the dimer formation. To test the native oligomeric state of ASPP2 Pro-Ank-SH3 we used AUC. Sedimentation equilibrium experiments showed that the protein was a monomer, with a molecular mass of  $43126 \pm 2047$  Da (Fig. 4D). This supports our idea that the residual dimer formation in the cross-linking experiments may be due to the experimental conditions, resulting in some intermolecular domain-domain interactions in addition to the intramolecular ones.

*The Sites in ASPP2 That Mediate the Domain-Domain Interaction*—To identify the precise residues in ASPP2 Pro and ASPP2 Ank-SH3, which mediate the domain-domain interaction, we designed membrane-bound peptide arrays containing partly overlapping peptides derived from the ASPP2 sequence (for peptide sequences see supplemental data). The peptide arrays were screened for binding the ASPP2 Pro and the ASPP2 Ank-SH3 domains. ASPP2 Pro-bound peptides from the first Ank repeat (aa 931–961) and from the SH3 domain (aa 1083–1096) (Table 1 and Fig. 5, A, B, and D). Screening a second peptide array revealed that ASPP2 Ank-SH3 bound several peptides derived from ASPP2 Pro (Table 2 and Fig. 5, C and D). These peptides are located between residues 693 and 752 at the N-terminal region of the ASPP2 Pro domain, and between residues 893 and 912 at its C terminus.

To quantify the binding of the ASPP2 Pro peptides to ASPP2 Ank-SH3, we synthesized fluorescein-labeled peptides derived from the overlapping binding sequences discovered in the peptide array and tested their binding to ASPP2 Ank-SH3 using fluorescence anisotropy. ASPP2 Ank-SH3 bound ASPP2 723–737 with a  $K_d = 16 \mu\text{M}$  (Fig. 5E) at physiological IS. Binding to ASPP2 693–712 was evident but did not reach saturation and was too weak to quantify (data not shown). ASPP2 739–752 and ASPP2 893–912 did not show any detectable binding to ASPP2 Ank-SH3 (data not shown). We analyzed the binding of ASPP2 723–737 to ASPP2 Ank-SH3 at different IS and found that the  $K_d$  at IS = 100 mM was  $5 \mu\text{M}$  and at IS = 50 mM was  $0.6 \mu\text{M}$  (Fig. 5E). The IS dependence of  $K_d$  indicates an electrostatic contribution to the interaction. We could not quantify the binding of the ASPP2 Ank-SH3 peptides to ASPP2 Pro, because of the instability of ASPP2 Pro that prevented us from reaching the high concentrations required for these studies.

*ASPP2 Ank-SH3 but Not ASPP2 Pro Mediates Interactions with Peptides Derived from ASPP2-binding Proteins*—To determine whether ASPP2 Pro is involved in the binding of ASPP2 to its partner proteins, we carried out another peptide array experiment. We designed an array of cellulose-bound partly overlapping peptides, derived from several proteins known to bind ASPP2 (Table 3, see supplemental data for peptide sequences). These proteins include the p65 subunit of NF $\kappa$ B (7), protein phosphatase 1 (8), HCV core protein (10), YAP1 (9) and the Bcl-2 family member Bcl-W.<sup>4</sup> The peptides were designed based on the domains in these proteins that are known to bind ASPP2 (Table 3). The peptides from YAP1 and HCV core protein were derived from short sequences already known to bind

<sup>4</sup> C. Katz, H. Benyamini, S. Rotem, and A. Friedler, unpublished results.

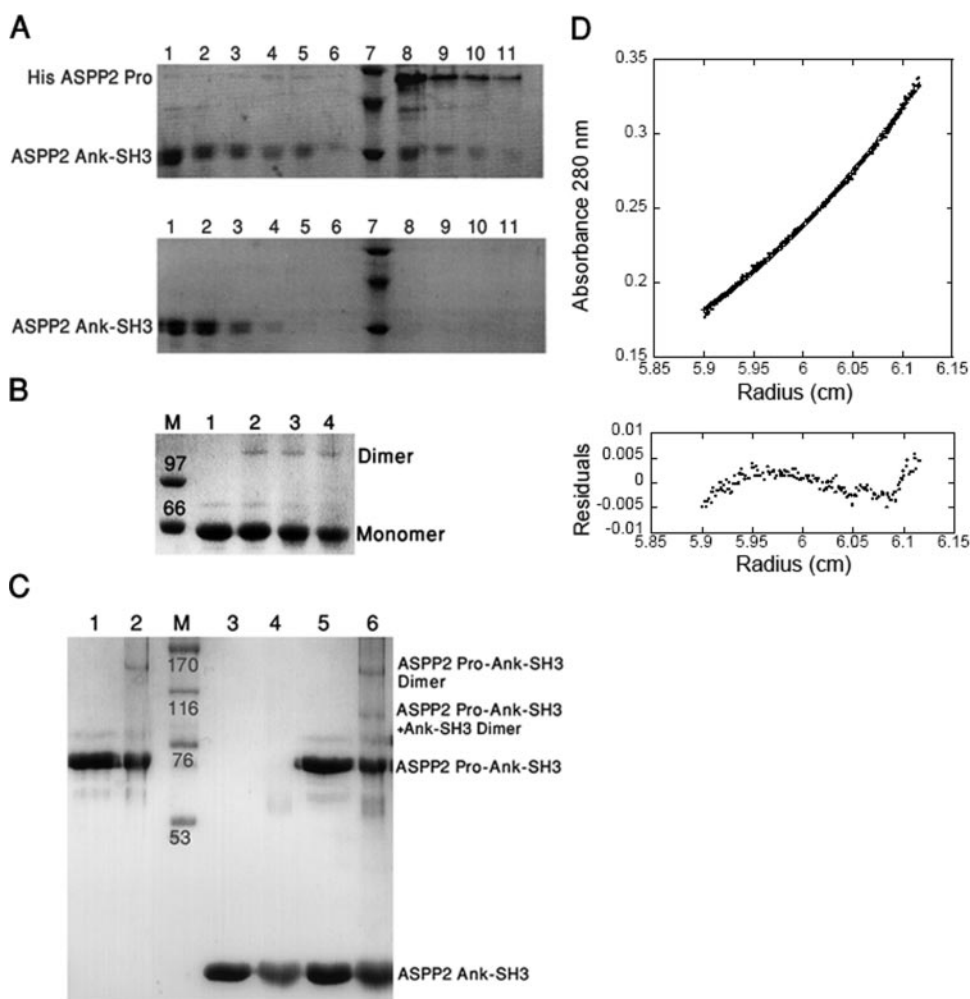


**FIGURE 4. Direct interaction between the ASPP2 Pro and ASPP2 Ank-SH3 domains.** *A*, nickel-affinity pull-down assay of ASPP2 Ank-SH3 by N-terminal His-tagged ASPP2 Pro. ASPP2 Ank-SH3 was incubated with His-tagged ASPP2 Pro (upper panel) or with wash buffer (lower panel) for 1 h at 4 °C and then incubated for another hour with nickel-NTA beads. The samples were centrifuged, and the suspension was kept (lane 1). The beads were washed with wash buffer containing 10 mM imidazole for five times (lanes 2–6), and then the proteins were eluted by the elution buffer, containing 250 mM imidazole, four times (lanes 8–11). ASPP2 Ank-SH3 was found in the elution fractions (8–11) only when incubated with ASPP2 Pro, but not with the buffer, indicating binding between the proteins. LMW (Amersham Biosciences) marker was used in lane 7. *B*, incubation of ASPP2 Pro-Ank-SH3 with different concentrations of the cross-linker BS3 resulted in some formation of dimers. Shown are the results for 25 equivalents of BS3 (lane 2), 50 equivalents of BS3 (lane 3), and 100 equivalents of BS3 (lane 4). No dimer was observed in the absence of the cross-linker (lane 1); *C*, incubation of ASPP2 Ank-SH3 with ASPP2 Pro-Ank-SH3 with or without BS3 (lanes 5 and 6), resulted also in some formation of a second type of dimer with a different molecular weight, corresponding to a dimer between ASPP2 Pro-Ank-SH3 and ASPP2 Ank-SH3. Incubation of ASPP2 Pro-Ank-SH3 with or without BS3 (lanes 1 and 2) and incubation of ASPP2 Ank-SH3 with or without BS3 (lanes 3 and 4) are shown as controls. *D*, AUC analysis of ASPP2 Pro-Ank-SH3 (top panel). Sedimentation equilibrium experiments shows that the protein is monomeric with molecular mass =  $43,126 \pm 2,047$  Da. The expected molecular mass of the protein is 48,300 Da. The bottom panel represents the residuals for the fit.

ASPP2 and served as positive controls (9, 10). We screened ASPP2 Pro and ASPP2 Ank-SH3 for binding the peptide array (Fig. 6). ASPP2 Pro did not bind the peptides in the array except for one positive spot, which is attributed to the YAP peptide that is known to bind this domain (Fig. 6A). ASPP2 Ank-SH3 bound to several peptides derived from each of the partner proteins (Fig. 6A and Table 3). The peptides from YAP1 and HCV core protein that served as positive controls indeed bound to ASPP2 Ank-SH3 in the array screening. The peptides from NF $\kappa$ B (p65), which we found to bind ASPP2, represent sites in NF $\kappa$ B that are known to mediate intermolecular interactions (Fig. 6B). The ASPP2 binding site between amino acids 303 and 355

corresponds to the known binding site for I $\kappa$ B, the natural inhibitor of NF $\kappa$ B, which contains ankyrin repeats like ASPP2 (47). The second ASPP2-binding site, between amino acids 21 and 50, is found in the DNA binding site of NF $\kappa$ B (48). We conclude that the proline-rich domain of ASPP2 is not involved in the interactions of ASPP2 with the partner proteins tested here. These interactions are mediated by ASPP2 Ank-SH3 domains.

*The ASPP2 Pro Domain Inhibits the Binding of ASPP2 Ank-SH3 to an NF $\kappa$ B Peptide*—To gain insight into the biological role of the domain-domain interaction in ASPP2, we tested whether binding of ASPP2 Pro to ASPP2 Ank-SH3 affects the intermolecular interactions mediated by ASPP2 Ank-SH3. As a model, we used the NF $\kappa$ B-derived peptide comprising residues 303–332, which was found to bind ASPP2 Ank-SH3 in the peptide array screening. We used fluorescence anisotropy to test the affinity of ASPP2 Ank-SH3 and ASPP2 Pro-Ank-SH3 to this peptide. ASPP2 Ank-SH3 bound NF $\kappa$ B 303–332 with  $K_d = 0.27 \mu\text{M}$ , whereas ASPP2 Pro-Ank-SH3 bound this peptide with  $K_d = 1.2 \mu\text{M}$ , an order of magnitude weaker (Fig. 7A). This shows that the presence of the proline-rich domain inhibits the interaction of ASPP2 Ank-SH3 with the NF $\kappa$ B peptide. Next, we tested by competition fluorescence anisotropy whether NF $\kappa$ B 303–332 and the ASPP2 Pro-derived peptide ASPP2 723–737 compete on the same binding site in ASPP2 Ank-SH3. When unlabeled ASPP2 723–737 was added to a pre-formed complex

of ASPP2 Ank-SH3 and fluorescently labeled NF $\kappa$ B 303–332 at IS = 50 mM, competition took place and the anisotropy decreased almost completely back to the initial values (Fig. 7B). The same trend was observed when the competition was performed in the opposite way: Unlabeled NF $\kappa$ B 303–332 displaced fluorescently labeled ASPP2 723–737 even quicker (Fig. 7C), because its affinity to ASPP2 Ank-SH3 was much tighter. As a control, we showed that there is competition between labeled and unlabeled ASPP2 723–737 (Fig. 7D). In summary, our results show that the interaction between ASPP2 Pro and ASPP2 Ank-SH3 inhibits the intermolecular interaction of the latter with the NF $\kappa$ B peptide.

**TABLE 1**
**Binding of ASPP2 Pro to ASPP2-derived peptides: screening of peptide array #1**

The peptides in this table, which were found to bind the ASPP2 Pro domains of ASPP2, are all derived from the Ank-SH3 domains of the protein. See Fig. 5A for screening results.

Peptide number	Binding residues	Sequence
14–15	931–961	LDSSLEGEFDLVQRIIYEVDPSLPNDEGIT
38	1083–1096	CMTIIHREDEDEIE

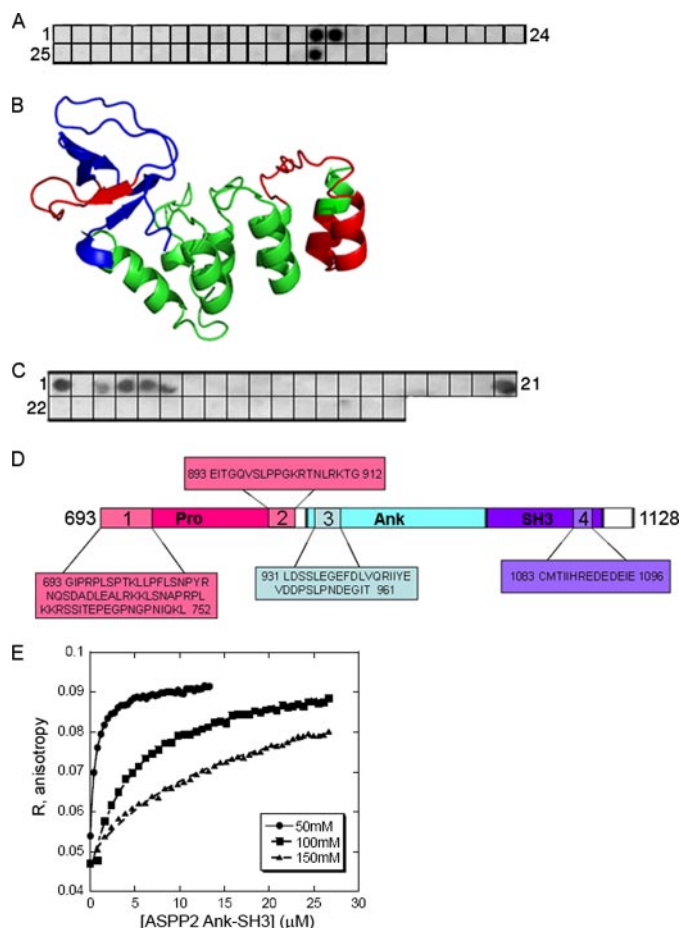


**FIGURE 5. The specific binding sites between the ASPP2 Pro and ASPP2 Ank-SH3 domains.** *A*, the sites in ASPP2 Ank-SH3 that bind ASPP2 Pro: An array consisting of peptides derived from ASPP2 was screened for binding ASPP2 Pro. Every *dark spot* represents binding between the corresponding peptide and ASPP2 Pro. For sequences of binding peptides see Table 1. For the complete peptide list see the supplemental data. *B*, the ASPP2 Pro binding sites in the ankyrin repeats (*green*) and the SH3 domain (*blue*) (coordinates taken from PDB id: 1YCS). The binding peptides are marked in *red*. *C*, the sites in ASPP2 Pro that bind ASPP2 Ank-SH3: An array consisting of peptides derived from ASPP2 was screened for binding ASPP2 Ank-SH3. Every *dark spot* represents binding between the corresponding peptide and ASPP2 Ank-SH3. For sequences of binding peptides see Table 2. *D*, a schematic diagram showing the different peptides in ASPP2 693–1128 that are involved in the domain-domain interactions. *E*, quantification of the binding of ASPP2 Ank-SH3 to peptides derived from the ASPP2 Pro domain: Binding of ASPP2 Ank-SH3 to fluorescein-labeled ASPP2 723–737 was studied using fluorescence anisotropy. ASPP2 Ank-SH3 bound ASPP2 723–737 with  $K_d = 16 \pm 1 \mu\text{M}$  at physiological IS. Binding was dependent on the IS, with  $K_d = 5 \mu\text{M}$  at IS of 100 mM and  $K_d = 0.6 \mu\text{M}$  at IS of 50 mM.

**DISCUSSION**

In the current study we performed detailed quantitative characterization of the structure and interactions of the ASPP2 Pro domain. We found that ASPP2 Pro is natively unfolded and

**TABLE 2**
**Binding of ASPP2 Ank-SH3 to ASPP2-derived peptides: screening of peptide array #2**

The peptides in this table, which were found to bind the ASPP2 Ank-SH3 domains of ASPP2, are all derived from the proline-rich domain of the protein. See Fig. 5C for screening results.

Peptide number	Binding residues	Sequence
1	693–712	I <sup>1</sup> PRPLSPTKLLPFLSNPYRN
3	713–732	QSDADLEALRKKLSNAPRPL
4	723–742	KKLSNAPRPLKKRSSITEPE
5	733–752	KKRSSITEPEGPNQNIQKL
21	893–912	EITGQVSLPPGKRTNLRKTG

**TABLE 3**
**Binding of ASPP2 Ank-SH3 to ASPP2-binding proteins: screening of peptide array #3**

The peptide array screening results are shown in Fig. 6.

ASPP2-partner protein	Residues in the partner protein	Binding peptides number	Binding residues
Bcl-W	1–188	5	10–35 57–86
p65 (NFκB) (7)	176–405	23–24	21–50
PP1 (8)	1–317	47–49	303–355
		58	19–48
		62	69–89
HCV core protein (10)	1–46	84–85	297–323
		86	1–20
		88	21–46
YAP1 (9)	84–208	89	81–100
		92	183–207

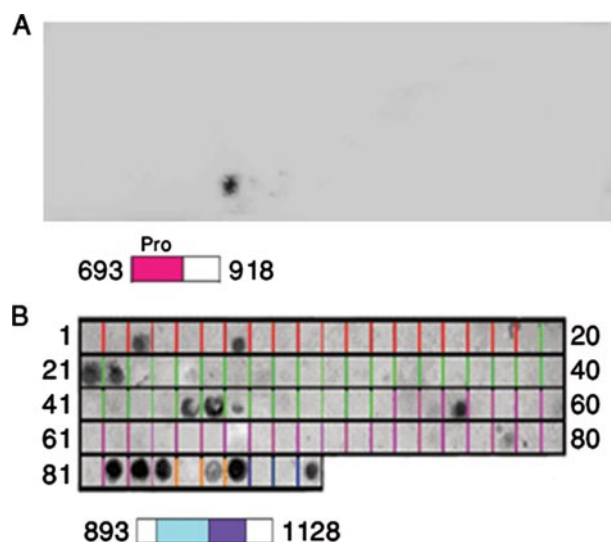


**FIGURE 6. Binding of ASPP2 to peptides derived from its binding proteins is mediated by ASPP2 Ank-SH3 but not by ASPP2 Pro.** A peptide array consisting of peptides derived from the ASPP2-binding proteins specified at Table 3 (Bcl-W in *red*, p65 in *green*, protein phosphatase 1 in *pink*, HCV core protein in *orange*, and YAP1 in *blue*) was screened for binding of ASPP2 Pro (*A*), which did not bind almost any of the peptides in the array and, ASPP2 Ank-SH3 (*B*). For sequences of binding peptides see Table 3. For the complete peptide list see the supplemental data.

that it binds the Ank-SH3 domains of ASPP2, but not peptides derived from ASPP2 binding proteins. The domain-domain interaction has a large inhibitory effect on the binding of ASPP2 Ank-SH3 to NFκB peptide. We suggest that the unstructured proline-rich domain of ASPP2 has a role in regulating the protein-protein interactions of ASPP2 by forming domain-domain interaction with the structured ASPP2 Ank-SH3.

*The Unstructured Nature of the ASPP2 Pro Domain*—Our results, obtained using CD, analytical gel filtration, and theoret-

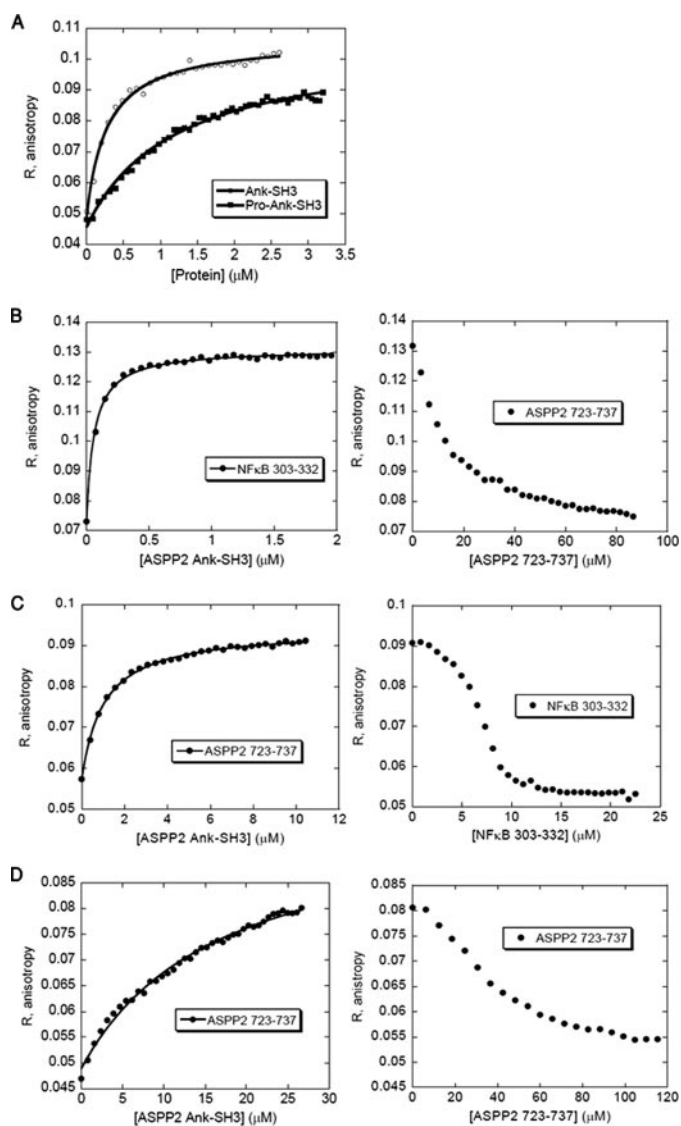


**FIGURE 7. ASPP2 Pro and NFκB 303-332 compete for the same binding site in ASPP2 Ank-SH3.** *A*, ASPP2 Ank-SH3 binds fluorescein-labeled NFκB 303-332 tighter than ASPP2 Pro-Ank-SH3: fluorescence anisotropy studies. ASPP2 Ank-SH3 bound NFκB 303-332 with  $K_d = 0.27 \mu\text{M}$ , whereas ASPP2 Pro-Ank-SH3 bound this peptide with  $K_d = 1.2 \mu\text{M}$ ; *B-D*: ASPP2 723-737 and NFκB 303-332 compete for binding ASPP2 Ank-SH3: fluorescence anisotropy competition experiments. *Left panel* in *B-D* shows the binding curves for the titration of ASPP2 Ank-SH3 into a fluorescein-labeled peptide, and the *right panel* describes the competition, where unlabeled peptide was titrated into the fully formed complex. Shown are the following competition experiments: unlabeled ASPP2 723-737 and fluorescein labeled NFκB 303-332 (*B*), unlabeled NFκB 303-332 and fluorescein labeled ASPP2 723-737 (*C*), and a control experiment of competition between unlabeled ASPP2 723-737 and fluorescein labeled ASPP2 723-737 (*D*).

ical predictions, are all consistent with the ASPP2 Pro domain being natively unfolded. There are also other known examples of unstructured proline-rich domains (49). In the analytical gel filtration experiments, the markers are globular folded proteins. An unfolded protein will elute earlier than expected, because it will not fit into the pores of the gel due to its extended conformation. This indeed was the case for ASPP2 Pro but not for the structured ASPP2 Ank-SH3.

ASPP2 belongs to the group of proteins that contain natively unfolded domains. Such domains thermodynamically favor an unstructured rather than a folded state. Almost 30% of the

eukaryotic genome encodes for proteins that are completely or partly unstructured (43, 50, 51). Natively unfolded proteins and protein domains are characterized by an almost complete lack of secondary and tertiary structure and an extended conformation with high flexibility (52). The lack of structure in natively unfolded proteins does not mean lack of function, and natively unfolded proteins present a case where the active state is unstructured (51, 53, 54). The structural flexibility of natively unfolded proteins and protein domains enables them to bind a large number of partner ligands by induction of folding (52). In our case, the natively unfolded ASPP2 Pro does not behave as a typical natively unfolded domain, because it does not interact with many proteins. On the contrary, our peptide array results (Fig. 6) as well as data in the literature about interactions between the full-length proteins (7–10) show that the Ank-SH3 domains are those that predominantly mediate the protein-protein interactions of ASPP2. If so, then what is the role of the proline-rich domain? Our data show that it is involved in an interaction with other ASPP2 domains: the ankyrin repeats and SH3 domain. We conclude that the ASPP2 Pro domain represents a unique case of a natively unfolded domain, because it mediates binding to another domain in the same protein but does not mediate almost any intermolecular interaction with the peptides and proteins tested so far (9).

*The Sites in ASPP2 That Mediate Domain-Domain Interaction*—We have mapped the sites in ASPP2 Pro that are involved in binding the ASPP2 Ank-SH3 domains and found four binding sequences that map to three regions in the proline-rich domain (Fig. 5D). The tightest binding peptide, spanning residues 723–737, lacks the typical PXXP motif and is one of the only positively charged segments (charge = +6) in the highly acidic 53BP2 region of ASPP2 ( $pI = 4.75$ ). The ionic strength dependence of the affinity of this peptide to ASPP2 Ank-SH3 indeed shows that there is a strong electrostatic contribution to the binding. Therefore, the overall binding between the domains could be initiated by an electrostatic attraction between the positive ASPP2 723–737 and the negative ASPP2 Ank-SH3, with subsequent fine-tuning of the interaction by the other ASPP2 Pro sequences involved. Additional binding peptides, which contain the PXXP motif, were identified in the peptide array screening but failed to show significant binding as free peptides in solution. It is possible that, although the binding of each of these peptides, which are not as positively charged as the 723–737 peptide, is weak, there is a cooperative effect within the full protein that promotes the binding.

The sites in ASPP2 Ank-SH3 that mediate the binding to ASPP2 Pro are located both in the SH3 domain and in the first ankyrin repeat (Fig. 5, *B* and *D*). SH3 domains are known to mediate protein-protein interactions by binding short proline-rich regions (45), which are characterized by the recurrence of the proline residue in the PXXP motif, where *X* is any amino acid (46). The ASPP2 Pro domain (aa 693–918) (Fig. 3D) contains 40 proline residues, including 7 repeats of the sequence PXXP. However, the site in the ASPP2 SH3 domain that we found to bind ASPP2 Pro includes the n-Src loop, but not the hydrophobic pocket, which usually mediates the interaction with PXXP motifs (55). This is not surprising, because the major

## Domain-Domain Interaction in ASPP2

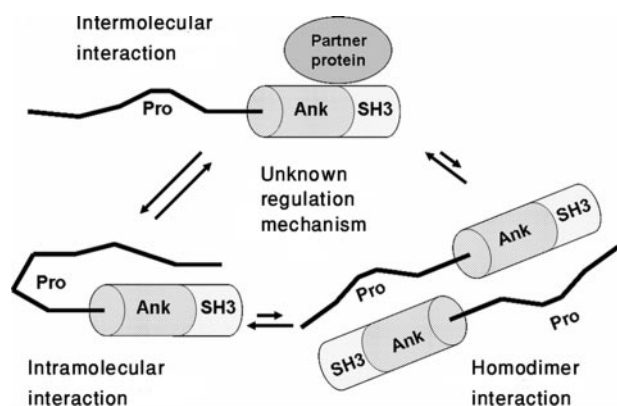


**FIGURE 8. A proposed mechanism by which the ASPP2 Pro domain regulates the protein-protein interactions of ASPP2.** The unstructured ASPP2 Pro domain binds the ASPP2 Ank-SH3 domains. This interaction could be either intramolecular within a given ASPP2 monomer, or intermolecular resulting in the formation of dimers. According to our results this equilibrium favors the intramolecular interaction and not dimerization. We propose that, by doing so, ASPP2 regulates its protein-protein interactions. The binding of the ASPP2 Pro domain to the ASPP2 Ank-SH3 domains blocks other protein-protein interactions that these domains mediate. Following a yet unknown control signal, the ASPP2 Pro domain is released from the ASPP2 Ank-SH3 domains, making them available to bind the partner proteins.

binding peptide from ASPP2 Pro is not a PXXP motif but a positively charged sequence.

*Is the Domain-Domain Interaction in ASPP2 Intra- or Intermolecular?*—In principle, the interaction between ASPP2 Pro and ASPP2 Ank-SH3 can be either intramolecular within a given ASPP2 monomer, or intermolecular, mediating dimerization of ASPP2 (Fig. 8). Our gel filtration and AUC experiments imply that ASPP2 Ank-SH3 and ASPP2 Pro-Ank-SH3 are monomeric (Fig. 3B, 4D). Moreover, our cross-linking experiments also resulted mainly in monomeric ASPP2 proteins. We think that cross-linking took place within a given monomer in these cases. However, we still observed residual dimerization for ASPP2 Ank-SH3, ASPP2 Pro-Ank-SH3, and a mixture of both. Dimerization in an ASPP family protein was recently observed also by Robinson *et al.* (6), who found that the Ank-SH3 domains of iASPP can form dimers within the crystal. The peptide responsible for dimerization was N-terminal to the ankyrin repeats, and its N terminus overlaps the C-terminal part of the iASPP proline-rich domain. This peptide also bound, among other sites, the n-Src loop of the SH3 domain, similar to what we found for ASPP2. It is possible that, also in iASPP, the full-length proline-rich domain forms additional interactions with the ankyrin repeats, which overlap the other interactions we discovered here for ASPP2 Pro, with the first ankyrin repeat. This may also explain why we observed a very small fraction of dimer following cross-linking of the ASPP2 Ank-SH3 with itself: similar to iASPP, the ASPP2 Ank-SH3 construct we used also contains the C terminus of the proline-rich domain (aa 893–918 in ASPP2). We conclude that, as was also proposed by Robinson *et al.* (6), dimerization in ASPP family proteins may not have physiological relevance and the residual interaction that they observed for iASPP (6) and we observed here for ASPP2 is due to experimental conditions. Still, this dimerization is possible, because the Ank-SH3 and Pro domains can interact with each other within a given monomer.

*Implications for Regulation and Function of ASPP2*—Based on our results, we propose a model according to which the interaction between the ASPP2 domains may serve as a control mechanism for regulating the interactions of ASPP2 with other proteins (Fig. 8). According to our model, the unfolded ASPP2 Pro domain, probably from the same ASPP2 monomer, wraps around the structured Ank and SH3 domains, preventing them from intermolecular binding to other proteins or to another ASPP2 molecule. When the ASPP2 Ank-SH3 domains are released from this interaction, following one or more as yet unknown control mechanisms, they are available for binding the specific target protein. Our results show that the presence of the proline-rich domain weakened the binding of the Ank-SH3 domains to a model target peptide derived from NF $\kappa$ B. These results support the model and confirm that the interactions of ASPP2 Ank-SH3 with ASPP2 Pro and with its binding proteins may take place via the same site.

The putative control mechanism that switches between the domain-domain and intermolecular interactions in ASPP2 could potentially involve post-translational modifications such as phosphorylations, because disorder-promoting residues are known to surround phosphorylation sites and it is assumed that protein phosphorylation occurs mainly within intrinsically disordered protein regions (56). Indeed, it was found that Bbp (ASPP2 123–1128) is phosphorylated and that constitutively active kinases weaken the interaction between YAP1 and Bbp *in vivo*, probably by phosphorylating Bbp (9). *In vitro*, various phosphopeptides derived from the YPPYPPPPYPS motif of ASPP2 (aa 866–876) also inhibit the interaction of Bbp with the YAP1 WW1 domain (9). ASPP2 423–848 was also found to be ubiquitinated, and its level is regulated by proteasomal degradation (57, 58). It is also possible that the interaction between ASPP2 Pro and ASPP2 Ank-SH3 also modulates the degradation of ASPP2.

Our model explains the reported observation that the interaction of Bbp and YAP1 *in vivo* was drastically increased when only the C-terminal part of Bbp (amino acids 852–1128, which is also the C-terminal part of ASPP2) was used (9). This C-terminal truncated form does not contain the regions in the proline-rich domain, which we found to bind the ASPP2 Ank-SH3 domains. Deletion of the proline-rich domain releases the Ank-SH3 domains from an intramolecular interaction, making it available to bind its target protein (YAP1 in this case).

Our study focused on the C-terminal part of ASPP2. We cannot exclude the possibility that the N-terminal domains of the protein also participate in intramolecular or intermolecular domain-domain interactions as a mechanism of regulating the activity of the protein. We are currently performing additional experiments to account for such possible interactions. In any case, the unfolded nature of the proline-rich domain makes it particularly suitable for interactions with other domains also in the context of the full-length protein.

Our results shed light on the structure and possible function of the ASPP2 Pro domain and extend the group of natively unfolded proteins. Future studies in cells will have to be performed to prove the proposed mechanism *in vivo* and to reveal the control mechanisms by which the domain-domain interaction in ASPP2 is regulated.

Acknowledgment—We thank Dr. Michal Goldberg for critical reading of the manuscript.

## REFERENCES

- Samuels-Lev, Y., O'Connor, D. J., Bergamaschi, D., Trigiant, G., Hsieh, J. K., Zhong, S., Campargue, I., Naumovski, L., Crook, T., and Lu, X. (2001) *Mol. Cell* **8**, 781–794
- Iwabuchi, K., Bartel, P. L., Li, B., Marraccino, R., and Fields, S. (1994) *Proc. Natl. Acad. Sci. U. S. A.* **91**, 6098–6102
- Naumovski, L., and Cleary, M. L. (1996) *Mol. Cell. Biol.* **16**, 3884–3892
- Tidow, H., Andreeva, A., Rutherford, T. J., and Fersht, A. R. (2007) *J. Mol. Biol.* **371**, 948–958
- Gorina, S., and Pavletich, N. P. (1996) *Science* **274**, 1001–1005
- Robinson, R. A., Lu, X., Jones, E. Y., and Siebold, C. (2008) *Structure* **16**, 259–268
- Yang, J. P., Hori, M., Takahashi, N., Kawabe, T., Kato, H., and Okamoto, T. (1999) *Oncogene* **18**, 5177–5186
- Helps, N. R., Barker, H. M., Elledge, S. J., and Cohen, P. T. (1995) *FEBS Lett.* **377**, 295–300
- Espanel, X., and Sudol, M. (2001) *J. Biol. Chem.* **276**, 14514–14523
- Cao, Y., Hamada, T., Matsui, T., Date, T., and Iwabuchi, K. (2004) *Biochem. Biophys. Res. Commun.* **315**, 788–795
- Bergamaschi, D., Samuels, Y., Jin, B., Duraisingham, S., Crook, T., and Lu, X. (2004) *Mol. Cell. Biol.* **24**, 1341–1350
- Lee, L. C., Hunter, J. J., Mujeeb, A., Turck, C., and Parslow, T. G. (1996) *J. Biol. Chem.* **271**, 23284–23288
- Sattler, M., Liang, H., Nettlesheim, D., Meadows, R. P., Harlan, J. E., Eberstadt, M., Yoon, H. S., Shuker, S. B., Chang, B. S., Minn, A. J., Thompson, C. B., and Fesik, S. W. (1997) *Science* **275**, 983–986
- Frank, R. (2002) *J. Immunol. Methods* **267**, 13–26
- Reineke, U., Volkmer-Engert, R., and Schneider-Mergener, J. (2001) *Curr. Opin. Biotechnol.* **12**, 59–64
- Reimer, U., Reineke, U., and Schneider-Mergener, J. (2002) *Curr. Opin. Biotechnol.* **13**, 315–320
- Rüdiger, S., Germeroth, L., Schneider-Mergener, J., and Bukau, B. (1997) *EMBO J.* **16**, 1501–1507
- Yu, G. W., Rüdiger, S., Veprintsev, D., Freund, S., Fernandez-Fernandez, M. R., and Fersht, A. R. (2006) *Proc. Natl. Acad. Sci. U. S. A.* **103**, 1227–1232
- Hansson, L. O., Friedler, A., Freund, S., Rüdiger, S., and Fersht, A. R. (2002) *Proc. Natl. Acad. Sci. U. S. A.* **99**, 10305–10309
- Mondigler, M., and Ehrmann, M. (1996) *J. Bacteriol.* **178**, 2986–2988
- Lucast, L. J., Batey, R. T., and Doudna, J. A. (2001) *BioTechniques* **30**, 544–546, 548, 550 passim
- Whitmore, L., and Wallace, B. A. (2004) *Nucleic Acids Res.* **32**, W668–W673
- Hayouka, Z., Rosenbluh, J., Levin, A., Loya, S., Lebendiker, M., Veprintsev, D., Kotler, M., Hizi, A., Loyter, A., and Friedler, A. (2007) *Proc. Natl. Acad. Sci. U. S. A.* **104**, 8316–8321
- Weinberg, R. L., Freund, S. M., Veprintsev, D. B., Bycroft, M., and Fersht, A. R. (2004) *J. Mol. Biol.* **342**, 801–811
- Friedler, A., Veprintsev, D. B., Freund, S. M., von Glos, K. I., and Fersht, A. R. (2005) *Structure* **13**, 629–636
- Liu, J., and Rost, B. (2003) *Nucleic Acids Res.* **31**, 3833–3835
- Ward, J. J., Sodhi, J. S., McGuffin, L. J., Buxton, B. F., and Jones, D. T. (2004) *J. Mol. Biol.* **337**, 635–645
- Li, X., Romero, P., Rani, M., Dunker, A. K., and Obradovic, Z. (1999) *Genome Inform. Ser. Workshop Genome Inform.* **10**, 30–40
- Linding, R., Russell, R. B., Neduva, V., and Gibson, T. J. (2003) *Nucleic Acids Res.* **31**, 3701–3708
- Yang, Z. R., Thomson, R., McNeil, P., and Esnouf, R. M. (2005) *Bioinformatics* **21**, 3369–3376
- Coeytaux, K., and Poupon, A. (2005) *Bioinformatics* **21**, 1891–1900
- Dosztanyi, Z., Csizsmok, V., Tompa, P., and Simon, I. (2005) *Bioinformatics* **21**, 3433–3434
- Wootton, J. C. (1994) *Comput. Chem.* **18**, 269–285
- Cheng, J., Sweredoski, M., and Baldi, P. (2005) *Data Mining and Knowledge Discovery* **11**, 213–222
- Obradovic, Z., Peng, K., Vucetic, S., Radivojac, P., and Dunker, A. K. (2005) *Proteins* **61**, Suppl. 7, 176–182
- Prilusky, J., Felder, C. E., Zeev-Ben-Mordehai, T., Rydberg, E. H., Man, O., Beckmann, J. S., Silman, I., and Sussman, J. L. (2005) *Bioinformatics* **21**, 3435–3438
- Zhao, L., O'Reilly, M. K., Shultz, M. D., and Chmielewski, J. (2003) *Bioorg. Med. Chem. Lett.* **13**, 1175–1177
- Hayouka, Z., Rosenbluh, J., Levin, A., Maes, M., Loyter, A., and Friedler, A. (2008) *Biopolymers (Peptide Science)*, in press
- Sanchez-Puig, N., Veprintsev, D. B., and Fersht, A. R. (2005) *Mol. Cell* **17**, 11–21
- Uversky, V. N., and Fink, A. L. (2002) *FEBS Lett.* **522**, 9–13
- Ferron, F., Longhi, S., Canard, B., and Karlin, D. (2006) *Proteins* **65**, 1–14
- Romero, P., Obradovic, Z., Li, X., Garner, E. C., Brown, C. J., and Dunker, A. K. (2001) *Proteins* **42**, 38–48
- Fink, A. L. (2005) *Curr. Opin. Struct. Biol.* **15**, 35–41
- Dyson, H. J., and Wright, P. E. (2005) *Nat. Rev. Mol. Cell. Biol.* **6**, 197–208
- Sparks, A. B., Rider, J. E., Hoffman, N. G., Fowlkes, D. M., Quillam, L. A., and Kay, B. K. (1996) *Proc. Natl. Acad. Sci. U. S. A.* **93**, 1540–1544
- Yu, H., Chen, J. K., Feng, S., Dalgarno, D. C., Brauer, A. W., and Schreiber, S. L. (1994) *Cell* **76**, 933–945
- Jacobs, M. D., and Harrison, S. C. (1998) *Cell* **95**, 749–758
- Chen, F. E., Huang, D. B., Chen, Y. Q., and Ghosh, G. (1998) *Nature* **391**, 410–413
- Dawson, R., Muller, L., Dehner, A., Klein, C., Kessler, H., and Buchner, J. (2003) *J. Mol. Biol.* **332**, 1131–1141
- Tompa, P. (2002) *Trends Biochem. Sci.* **27**, 527–533
- Dunker, A. K., Lawson, J. D., Brown, C. J., Williams, R. M., Romero, P., Oh, J. S., Oldfield, C. J., Campen, A. M., Ratliff, C. M., Hipps, K. W., Ausio, J., Nissen, M. S., Reeves, R., Kang, C., Kissinger, C. R., Bailey, R. W., Griswold, M. D., Chiu, W., Garner, E. C., and Obradovic, Z. (2001) *J. Mol. Graph. Model.* **19**, 26–59
- Wright, P. E., and Dyson, H. J. (1999) *J. Mol. Biol.* **293**, 321–331
- Uversky, V. N. (2002) *Protein Sci.* **11**, 739–756
- Cherny, I., Rockah, L., and Gazit, E. (2005) *J. Biol. Chem.* **280**, 30063–30072
- Kay, B. K., Williamson, M. P., and Sudol, M. (2000) *FASEB J.* **14**, 231–241
- Iakoucheva, L. M., Radivojac, P., Brown, C. J., O'Connor, T. R., Sikes, J. G., Obradovic, Z., and Dunker, A. K. (2004) *Nucleic Acids Res.* **32**, 1037–1049
- Zhu, Z., Ramos, J., Kampa, K., Adimoolam, S., Sirisawad, M., Yu, Z., Chen, D., Naumovski, L., and Lopez, C. D. (2005) *J. Biol. Chem.* **280**, 34473–34480
- Sullivan, A., and Lu, X. (2007) *Br. J. Cancer* **96**, 196–200